THE INTERNATIONAL JOURNAL OF
DEVELOPMENTAL
BIOLOGY
www.intjdevbiol.com

Light microscopy of mammalian gametes and embryos: methods and applications

ANNA AJDUK*,1 and MACIEJ SZKULMOWSKI[2]

1Department of Embryology, Faculty of Biology, University of Warsaw, Warsaw and
2Institute of Physics, Faculty of Physics, Astronomy and Informatics, Nicolaus Copernicus University, Torun, Poland

ABSTRACT In recent years, we have witnessed an unprecedented advancement of light microscopy techniques which has allowed us to better understand biological processes occurring during oogenesis and early embryonic development in mammals. In short, two modes of cellular imaging are now available: those involving fluorescent labels and those which are fluorophore-free. Fluorescence microscopy, in its various forms, is used predominantly in research, as it provides detailed information about cellular processes; however, it can involve an increased risk of photodamage. Fluorophore-free techniques provide, on the other hand, a smaller amount of biological data but they are safer for cells and therefore can be potentially used in a clinical setting. Here, we review various fluorescence and fluorophore-free visualisation approaches and discuss their applicability in developmental biology and reproductive medicine.

KEY WORDS: *microscopy, fluorescence, oocyte, spermatozoa, embryo*

Introduction

The first attempts to magnify objects of interest date back to ancient times. The observation that objects appear enlarged when seen through a spherical shaped glass vessel was most likely an accidental discovery. It took hundreds of years until the first practical application of this phenomenon, i.e. eyeglasses, was invented (in the 13th century). Then it took another 300 years before the invention of other aids to vision, a telescope and a microscope (around 1600, the exact date unknown). The earliest known examples of compound microscopes, combining an objective lens positioned near the specimen with an eyepiece, appeared in Europe around 1620. The first microscopic observations of cells were done in the 17th century by Robert Hooke (1635-1703) and continued by Antonie van Leeuwenhoek (1632-1723) (Bardell, 2004).

Since the 17th century our understanding of the nature of light and ways to harness it in order to visualize the micro-world has progressed enormously. Particularly impressive advancement in imaging techniques has been made in the recent decades, when different types of microscopes utilizing linear and non-linear optics have been constructed, allowing us to look into cellular architecture deeper than ever before. One of the biological disciplines that has profited a lot from the improvement of imaging techniques is developmental and reproductive biology of mammals.

Mammalian oocytes are relatively big cells with a diameter in range of 70-120 μm (at least in species examined so far; Griffin *et al.*, 2006). Spermatozoa, in terms of volume, are orders of magnitude smaller, but possess a long tail, and therefore reach in most mammalian species a total length of 50-100 μm (Cummins and Woodall, 1985). Preimplantation embryos are initially the same size as oocytes, which means that with every division the size of single cells (blastomeres) decreases. At the late blastocyst stage embryos start to expand and their growth continues after implantation (Fig. 1A). The large size of oocytes and preimplantation embryos, combined with the cytoplasm that in many species, including mouse and human, is translucent, make them an attractive object for visualisation. Indeed, quite a lot of information about oocyte/embryo morphology, such as number of nuclei, cytoplasm granulation, size and shape of blastomeres, etc. can be derived

---

*****Address correspondence to:** Anna Ajduk. Department of Embryology, Faculty of Biology, University of Warsaw, Miecznikowa 1, 02-096 Warsaw, Poland.
Tel.: +48-22-5541212. Fax.: +48-22-5541210. E-mail: aajduk@biol.uw.edu.pl - (iD) https://orcid.org/0000-0002-7262-1370
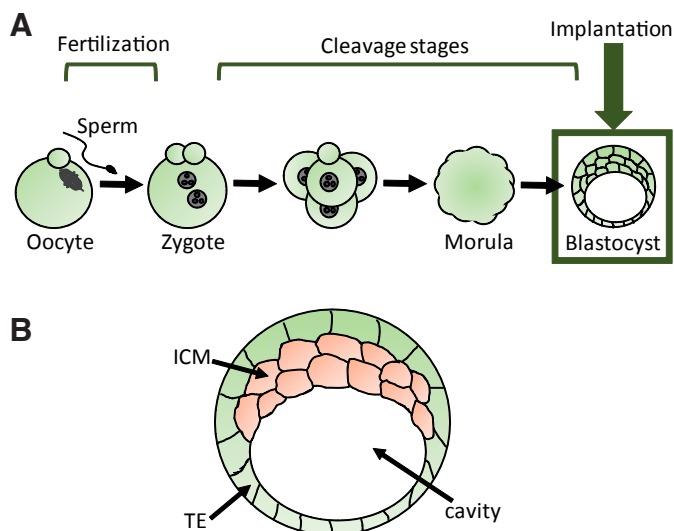
Fig. 1. The main stages of preimplantation development of a mammalian embryo. (A) *Fertilization of an oocyte arrested in metaphase of the 2nd meiotic division induces completion of the oocyte's meiosis and activation of embryonic development. During the next few days (e.g. 4-5 days in mouse, 5-6 days in human), the embryo undergoes a series of mitotic divisions (so-called cleavage divisions) that transform the 1-cell embryo (zygote) into a multicellular structure: first, a morula, containing approx. 16 cells, and then a blastocyst, built of tens of cells forming a sphere with a cavity inside. A blastocyst stage is the last one that can be easily cultured outside the female body, as blastocysts need to implant in the uterus to develop further.* **(B)** *In a blastocyst we can distinguish an inner cell mass (ICM), i.e. a group of cells that give rise to the future embryo proper and some of the extraembryonic membranes, and a trophectoderm (TE), a layer of cells surrounding the ICM and the blastocyst cavity, that will form a foetal part of the placenta.*

simply from bright field images. Even today this kind of imaging is used in assisted reproduction to assess quality of gametes and embryos (Ebner *et al.*, 2003; Ajduk and Zernicka-Goetz, 2013; Omidi *et al.*, 2017 and references therein).

However, if we wish to look deeper into cellular physiology of gametes or embryos and visualise particular molecules or organelles, imaging becomes more complicated. Initially, a more detailed visualisation of the intracellular structures was limited almost exclusively to fixed specimens subjected to immunofluorescence staining, so information about spatiotemporal dynamics of cellular processes was difficult to extract. It has been changed by two inventions. First, advancements in molecular biology allowed expression of fluorescently-tagged proteins in gametes and embryos and therefore visualisation of their dynamic distribution in live cells. Second, reliable and easy-to-use time-lapse imaging systems have been developed, providing an appropriate environment for live oocytes and embryos during imaging. Microscopes have been combined with environmental chambers that ensure the optimal culture conditions, i.e. constant temperature and pH of the medium. A significant advancement in microscopy technology has also permitted a decrease in illumination (oocytes and embryos are very light-sensitive) without sacrificing quality of the obtained images.

In the present review we wish to discuss how mammalian gametes and preimplantation embryos can be visualized either in research or a clinical setting. In general, we distinguish two modes of imaging: requiring fluorescent labels and fluorophore-free. Fluorescence microscopy, in its various incarnations, is used almost exclusively in research, as it is very effective in visualizing cellular processes in a great detail, but brings an increased risk of photodamage. Fluorophore-free techniques provide, on the other hand, lower amount of biological information but are considered safer for cells and therefore are used mainly, although not exclusively, in a clinical setting. What parameters define usability of different imaging techniques? What are their advantages and limitations, current applications and future perspectives? These are the questions we address below (see also the summary in Table 1).

Not just a pretty image – fluorescence microscopy

Fluorescence microscopy exploits the phenomenon that certain molecules (fluorophores) immediately after light absorption emit light with spectrum shifted towards longer wavelengths. In fluorescence microscopes the sample is illuminated by light of a defined wavelength close to the peak of the excitation spectrum of either intrinsic fluorophores present in the sample (autofluorescence) or of fluorescently labelled proteins (or other molecules). Then, the light emitted by the fluorophores is detected. This mode of action is its main advantage and, at the same time, its greatest vice. It allows to examine with a submicrometer resolution localization of fluorescently labelled molecules, organelles or whole cells and, if combined with time-lapse imaging, also their spatiotemporal dynamics and functions. Therefore it is a great source of information about various biological processes occurring in cells, tissues or even whole organisms. On the other hand, high-intensity light required for fluorescence microscopy is damaging to cells, both through its direct effect on biological macromolecules (especially the near-UV range that can induce DNA damage), and through fluorophore photobleaching. Each time a fluorescent sample is illuminated, a fraction of the fluorophore population is destroyed and free radicals and other highly reactive breakdown products are generated. The degree of phototoxicity differs depending on the fluorophore e.g., fluorescent proteins tend to be less phototoxic compared to chemical fluorescent dyes because the reactive part of the protein responsible for emitting light and sensitive to photobleaching is contained within a rigid beta-barrel structure (Kremers *et al.*, 2011). The only certain way to reduce photobleaching and associated photodamage is to reduce the irradiation exposure by limiting exposure time and light intensity as much as possible while retaining a sufficient signal-to-noise ratio required for the specific experimental questions.

We can distinguish two types of fluorescence imaging: widefield epifluorescence microscopy and confocal microscopy. Widefield illumination allows for a faster (and therefore less damaging) image acquisition - the entire field of view is excited at once with light produced by a lamp (e.g. mercury, xenon, tungsten or LED) and filtered by an excitation filter. However, the in-focus features are obscured by a blur from out-of-focus regions of the sample, and this limits the quality of the image if the sample thickness is more than 15–20 μm. On the other hand, in laser scanning confocal microscopy (LSCM) an image is generated by a focused laser beam scanning across the sample and the emitted fluorescence is filtered by a confocal pinhole, suppressing out-of-focus light and allowing for optical sectioning of thick samples and significantly improving

TABLE 1

THE MAIN FEATURES OF VARIOUS MICROSCOPY TECHNIQUES

Type of microscopy	Main features	References
Fluorescence microscopy		
Widefield fluorescence	• Lateral resolution of ~200 nm • Axial resolution of ~500 nm • Image acquisition of 10-1000 Hz • Blur caused by the out-of-focus light • Large field of view • Photodamage/ bleaching outside of the imaged area	Ettinger and Wittman, 2014 Sanderson *et al.,* 2014
Laser scanning confocal	• Lateral resolution of ~200 nm • Axial resolution od ~100 nm • Relatively low imaging speed (~0.5-10 Hz with galvanometer scanners and 10-30 Hz with resonant scanners) • Small field of view • Photodamage/bleaching outside of the imaged area (in z axis) • Adaptation of image size vs. imaging speed •	Ettinger and Wittman, 2014 Jonkman *et al.,* 2014 Sanderson *et al.,* 2014
Spinning disc confocal	• Lateral resolution of ~200 nm • Axial resolution od ~100 nm • High imaging speed (1000 Hz) • Lower illumination – reduced photobleaching • Non-uniform illumination profile compromising quantitative imaging techniques • Fixed magnification • Non-adjustable pinhole size preventing optimization of optical sectioning and resolution	Graf *et al.,* 2005 Oreopoulos *et al.,* 2014 Sanderson *et al.,* 2014
Two-photon	• Lateral resolution of ~250 nm • Axial resolution od ~150 nm • Penetration depth higher than in one photon microscopy • Low background signal (no excitation outside the focal plane) • Low photobleaching and phototoxicity • Signal to noise ratio lower than in one photon microscopy • A pulsed laser required	Denk *et al.,* 1990 Helmchen and Denk, 2005 Sanderson *et al.,* 2014
Superresolution	• Lateral resolution: SIM – 50-100 nm, STED - < 50 nm, STORM - ~ 20-30 nm, PALM - < 20 nm • Axial resolution: SIM – 50-100 nm, STED - ~ 150 nm, STORM - ~ 50 nm, PALM - ~ 30 nm • Low imaging speed: SIM, STED 0.05-0.1 Hz, STORM – 0.5-1 Hz • In SIM and STED traditional dyes may be used, but STORM and PALM require special fluorophores • Technically complicated (STED) • STORM and PALM limited to fixed cells, SIM compatible with fixed and live cell imaging	Hell and Wichmann, 1994 Heintzmann and Jovin, 2002 Betzig *et al.,* 2006 Rust *et al.,* 2006 Hein *et al.,* 2008 Yamanaka *et al.,* 2008 Leung and Chou, 2011 Allen *et al.,* 2013 Fiolka, 2014 Sanderson *et al.,* 2014 Shtengel *et al.,* 2014
Light sheet	• Axial and lateral resolution of 300 nm • Imaging speed of ~ 15 Hz • Illumination only in the focal plane • Can be easily combined with SIM • Matches resolution of confocal microscopy only after deconvolution • Produces huge data-sets - difficult data storage and analysis	Voie *et al.,* 1993 Keller and Stelzer, 2008 Santi, 2011 Weber *et al.,* 2014
Fluorophore-free microscopy		
Differential interference contrast / Phase contrast	• Lateral resolution of ~ 200 nm • Axial resolution of ~ 500 nm • No fluorophore required • Provides low amount of biological information	Salmon and Tran, 1998 Centonze Frohlich, 2008
Polarized light	• Lateral resolution of ~ 200 nm • Axial resolution of ~ 500 nm • No fluorophore required • Only birefringent structures can be visualised	Oldenbourg and Mei, 1995 Inoue, 2002 Oldenbourg, 2013
Harmonic generation	• Axial and lateral resolution of 500-700 nm (for second harmonic generation) and 400 nm (for third harmonic generation) • Imaging speed of 0.4-4 Hz • No energy deposition in the sample • No fluorophore required • High penetration depth • Sensitive to optical aberrations • Only certain types of structures can be visualized	Sun *et al.,* 2004 Watanabe *et al.,* 2010 Cox, 2011
Optical coherence microscopy	• Axial and lateral resolution of 1-2 μm • Imaging speed of approx. 3 Hz per 3D image (depending on the volume size), 100 kHz-10 MHz linear • Low energy deposit: infrared light illumination and short exposures per beam position on the sample. • No fluorophore required • Very well suited for a volumetric imaging • Produces huge data-sets - difficult data storage and analysis • Requires significant amount of data processing • Requires sophisticated algorithms to obtain uniform resolution in the whole imaging volume	Hoeling *et al.,* 2000 Latrive and Boccara, 2011 Liu *et al.,* 2014 Karnowski *et al.,* 2017
Raman spectro-microscopy	• Axial and lateral resolution of 1 μm • Imaging speed of 50 Hz • Allows label-free analysis of the sample chemical content • Only molecules with a vibrational spectrum can be imaged	Zumbusch *et al.,* 2013

three-dimensional (3D) spatial resolution. LSCM has however few limitations. A laser beam is deflected by a pair of galvanometer mirrors (see Box 1) and scans the sample pixel by pixel in a linear raster mode, which slows down the image acquisition to typically 500 ms to 2 s per image, depending on the image dimensions. Moreover, the sample is subjected to a relatively high irradiation in order to increase the emitted signal, as only part of the emitted light (only the fluorescence produced in the focal plane) is directed to the detector; the rest is rejected by the confocal pinhole. The third disadvantage is depth of penetration, which with 100 μm is significantly better than in widefield microscopy, but still not sufficient in certain applications (Canaria and Lansford, 2010; Ettinger and Wittman, 2014).

The issue of a slow scanning speed in LSCM has been at least partially addressed by an introduction of resonant scanning mirrors (Box 1) that are capable of gathering images at 15 to 30 frames per second (fps) for 1024x1024 pixels or 512x512, respectively, or even up to 420 fps for smaller images.

Spinning disc confocal microscopy (SDCM), on the other hand, presents a solution to the specimen irradiance issue. Instead of slow raster scanning, in SDCM the excitation light is spread over thousands of pinholes that scan across the specimen rapidly (Petran *et al.*, 1968) and are registered simultaneously with charge-coupled device (CCD) cameras, which are more sensitive than photomultiplier tubes or avalanche photodiodes used in LSCM (Box 1). This greater detection sensitivity reduces the exposure times required in SDCM experiments and diminishes the amount of irradiance that reaches each particular point in the sample and inflicts markedly less photobleaching compared to LSCM. Additionally, due to a parallel detection with CCD cameras, it permits a much faster image acquisition. These features make SDCM especially well-suited for live-cell imaging. However, quantitative imaging techniques, like colocalization or Förster resonance energy transfer (FRET), are often compromised by the non-uniform illumination profiles of SDCM. SDCM lacks also the ability to adjust the pinhole size to optimize the optical sectioning or resolution (Oreopoulos *et al.*, 2014).

Two-photon microscopy (2PM) also solves some issues of traditional LSCM. In 2PM microscopy, two near-infrared photons are absorbed simultaneously by a fluorophore that normally absorbs a shorter wavelength of light (Denk *et al.*, 1990). As in LSCM, the image is obtained by raster scanning the focused beam over the sample while collecting the emitted fluorescence into a detector. Since two-photon absorption is non-linear and occurs dominantly in the focal volume, where high photon densities are reached, 2PM has an intrinsic 3D resolution without the need of a detection pinhole. In turn, the efficiency of signal acquisition is improved, since light generated in the focal volume and subsequently scattered within the sample is not rejected. Moreover, compared to LSCM, 2PM imaging benefits from a lower cellular toxicity (as near-infrared light utilized in 2PM interacts less with biological samples) and a superior depth of penetration (also due to the usage of near-infrared light) (Denk *et al.*, 1990, Canaria and Lansford, 2010). It can be combined with a resonant scanning mode to increase the speed of image acquisition.

Fluorescence microscopy, both widefield and confocal, has become an indispensable tool in cell biology of mammalian gametes and embryos: in the last 20 years it is difficult to find a publication without data acquired by one of these imaging techniques. Even

simple observations regarding localization of certain molecules/organelles in gametes or blastomeres may have deep scientific consequences, as they indicate asymmetries inside and between cells and reflect their differentiation status (Ajduk and Zernicka-Goetz, 2016; White *et al.*, 2018). Combined with time-lapse imaging equipment, advanced image analysis, and, last but not least, molecular biology and micromanipulation techniques allowing expression of fluorescently tagged proteins in gametes and embryos, fluorescence microscopy revealed how oocytes react on a molecular level to fertilization (e.g., Cuthbertson and Cobbold, 1985; Saunders *et al.*, 2002, Madgwick *et al.*, 2006; Ajduk *et al.*, 2011), how oocyte and blastomere divisions are regulated both temporally and spatially (e.g., Schuh and Ellenberg, 2008; Ajduk *et al.*, 2014, 2017; Strauss *et al.*, 2018), or how developmental fates of blastomeres within the embryo are decided (e.g., Morris *et al.*, 2010; Parfitt and Zernicka-Goetz, 2010; Anani *et al.*, 2014; Samarage *et al.*, 2015). Additionally, a repertoire of phenomena that can be examined with fluorescence microscopy is extended by accompanying quantitative methods such as Förster resonance energy transfer (FRET), fluorescence recovery after photobleaching (FRAP) or fluorescence decay after photoactivation (FDAP). FRET relies on a distance-dependent energy transfer between two light-sensitive molecules: if both molecules are in a very close proximity, an excited donor fluorophore may transfer energy to an acceptor fluorophore that starts emitting light. FRET-compatible sensors has been applied to follow intracellular dynamics of small molecule signal mediators (e.g., cGMP, cAMP, InsP$_3$, NO) in gametes and embryos (Manser and Houghton, 2006; Shirakawa *et al.*, 2006; Shuhaibar *et al.*, 2015; Mukherjee *et al.*, 2016) or interactions between proteins in a sperm head, an oocyte spindle or embryonic nuclei (Baluch *et al.*, 2004; Baluch and Capco, 2008; Bogolyubova *et al.*, 2013; Andrews *et al.*, 2015). FRAP, on the other hand, determines kinetics of diffusion through tissues or cells. Fluorophores in the region of interest are bleached with a high intensity laser beam,

and a diffusion rate of still-fluorescent probes from other parts of the sample into the bleached area are measured. FRAP is used in research on cell-to-cell communication in ovarian follicles (Santiquet *et al.*, 2012), dynamics of oocyte/embryo cytoskeleton (Azoury *et al.*, 2008; 2011) and chromatin (Bošković *et al.*, 2014; Ooga *et al.*, 2016; Ooga and Wakayama, 2017) or mobility of specific molecules within sperm plasma membranes (Schröter *et al.*, 2016; James *et al.*, 2004). FDAP acts reversely to FRAP: laser beam photoactivates fluorophores in the region of interest and then a rate of their translocation out of the region is analysed. This method was used to examine dynamics of interactions between transcription factors and chromatin in blastomeres (Plachta *et al.*, 2011).

As our knowledge about cells extends, the need for a higher resolution, providing even more detailed information about molecular processes and interactions in cells, increases as well. The spatial resolution of traditional fluorescence microscopes is limited by diffraction to approximately 200 nm in xy-dimensions and 500 nm along the optical axis. In the last 15 years we witnessed the emergence of various superresolution fluorescence methods, i.e. techniques that break the diffraction limit (see Box 2) and image samples at length scales considerably lower than the wavelength of visible light. In some of them, such as photoactivated localization microscopy (PALM) (Betzig *et al.*, 2006) and stochastic optical reconstruction microscopy (STORM) (Rust *et al.*, 2006) the diffraction limit is overcome by taking advantage of photoswitchable molecules that can be stochastically switched on and off depending on the wavelength of the incident light. By imaging only a small fraction of non-overlapping, stochastically activated fluorophores at a time and localizing their positions, subdiffraction images can be reconstructed with approximately 20 nm lateral and 50 nm axial

Box 2. An optical glossary

Birefringence – an optical property of some materials, where a refractive index of a material depends on the polarization and direction of light.
Diffraction limit – the principal limit of optical resolution for a given optical system, the minimal spot size the system can produce when all aberrations are neglected. The spot size is proportional to the wavelength (shorter wavelengths give better resolution) and inversely proportional to the numerical aperture of the objective lens (higher NA gives better resolution).
Moiré pattern – a low frequency fringe pattern that appears when two fringe patterns with higher and similar frequencies, differing in orientation, alignment or frequency distribution, are overlaid.
Interference fringe – a result of superposition of two beams of coherent light. Due to constructive and destructive interference, it consists of alternated bright and dark bands.
Raman scattering – an inelastic scattering of photons that causes the scattered photon to have different energy than the incident photon. In so-called Stokes Raman scattering the scattered photons have lower energy, while in anti-Stokes Raman scattering the scattered photons have higher energy than the incident photons. This phenomenon can be used in spectroscopy, as the spectrum of scattered light depends on the scattering molecules.
Refractive index – describes how fast light propagates through a material. It is calculated as a ratio between speed of light in a vacuum and in the examined material.
Second / third harmonic generation – a nonlinear optical phenomenon, where a single photon with a shorter wavelength (and doubled or tripled energy) is created from two or three low energy photons.

resolution. However, these so called single molecule localization microscopy methods generally have poor temporal resolution and are typically performed on fixed cells due of the necessity of acquiring large image sequences in order to faithfully reconstruct the sample at high resolution (reviewed in Allen *et al.*, 2013). Despite this limitation, they have been used to image mammalian gametes/embryos, especially to visualize 3D ultrastructure of spermatozoa (Chung *et al.*, 2014; Gervasi *et al.*, 2018) or chromatin structure in oocytes (Prakash *et al.*, 2015; Agostinho *et al.*, 2018). An alternative scanning-based approach, stimulated emission depletion (STED) microscopy, uses a second laser with an engineered doughnut shape de-excitation spot to reduce the area where the fluorescence induced by the excitation laser occurs. It effectively increases the resolution of the point-scanned image (Hell and Wichmann, 1994) and has been applied in sperm research (Ito *et al.*, 2015). Another popular superresolution approaches rely on structured illumination to break the diffraction barrier (Fiolka, 2014). In the widefield approach called structured illumination microscopy (SIM), a number of patterns of spatially modulated excitation light is superimposed on the sample while imaging. As a result, sample features that are normally beyond the resolution of the microscope appear in the form of Moiré pattern (Box 2) and become detectable. Through a rotation and translation of the illumination patterns, followed by a numerical image reconstruction procedure, superresolution images are obtained at approximately half of the diffraction limit. Structured illumination techniques are compatible with both fixed- and live-cell imaging and have been used to examine mechanism of an acrosome reaction or interactions between sperm and microvesicles (Al-Dossary *et al.*, 2015; Sharif *et al.*, 2017).

Although techniques mentioned above are sufficient for most experimental set-ups when gametes or preimplantation embryos are considered, they are not always suitable for larger specimens. Therefore, to extend research to peri- and postimplantation stages and follow processes such as gastrulation or organogenesis another approach has to be taken. Light sheet microscopy (LSM), also known as a selective plane illumination microscopy (Huisken *et al.*, 2004, Keller *et al.*, 2008), is compatible with low-NA, low magnification, and long-working-distance objectives. In this technique, paths of illumination and fluorescence light detection are decoupled and are perpendicular to each other. The sample is illuminated with a sheet of light formed by optics with a low-NA, as compared to optics in the detection path, and the fluorescence is generated in a few µm thick slice, which is then imaged with the higher NA optics and recorded by a CCD camera. In this unique optical arrangement, unlike in typical confocal microscopy, optical sectioning is achieved directly across the entire plane and the image is recorded in a single exposure. Each pixel of the CCD camera collects photons for the entire duration of the exposure time, up to tens of milliseconds. In contrast, in a standard confocal microscope, the scanner needs to move from one pixel to the next and can only rest in each point for few microseconds. Hence, the parallel recording of all pixels in LSM is much more efficient and the local excitation intensity can be kept very low. In combination with fast and sensitive cameras, it enables rapid acquisition of large image datasets while still offering a superior signal-to-noise ratio and minimal phototoxicity (Weber *et al.*, 2014). LSM has a lower spatial resolution compared to standard confocal microscopy, but when combined with a multiview approach (when a number of light illumination directions is used) almost isotropic resolution is achiev-

able, making the images susceptible to deconvolution (Verveer *et al.*, 2007). LSM is best suited to follow dynamic developmental processes in postimplantation embryos and foetuses (Ichikawa *et al.*, 2014; Udan *et al.*, 2014; Belle *et al.*, 2017), although there are also reports describing its use for preimplantation embryos (Strnad *et al.,* 2016; de Medeiros *et al.*, 2016).

No label, no cry – fluorophore-free microscopy

Although fluorescence microscopy has provided us with an enormous amount of information regarding cellular structure and molecular processes occurring in cells, it is inevitably burdened with a risk of inflicting photodamage. The risk can be minimized by optimization of the imaging set-ups, so it does not disturb experimental procedures, but even then it still remains unacceptable in some applications, such as quality assessment of gametes and embryos in assisted reproduction. Therefore, in addition to optimizing fluorophore-based approaches, label-free optical techniques are also developed.

Many linear label-free optical microscopy techniques have been widely used for decades, a good example being differential interference contrast (DIC) microscopy and phase contrast microscopy. The contrast in these techniques relies on refractive index differences in the sample (Box 2). They introduce phase shifts between light scattered by the sample and the unaltered illumination light that diversify intensity of the detected signal (Zernike, 1935). They are used in assisted reproduction laboratories to visualize morphology of gametes and developing embryos, aiding to select those of the highest developmental potential. The oldest, but still very popular in *in vitro* fertilization (IVF) clinics, procedure of gamete/embryo scoring is based simply on static 'snapshot' observations: gametes/embryos are screened for specific morphological features at certain time-points of their culture. In case of oocyte scoring, parameters such as cytoplasm granulation, size of the previtaline space, presence of the 1st polar body or morphology of the zona pellucida are analysed. In sperm assessment, morphology of the sperm nucleus, acrosome, neck and tail, as well as number and size of vacuoles in the sperm head, are usually taken into consideration. After fertilization, embryos are graded according to morphology of the cytoplasm and pronuclei, including number and distribution of the nucleoli (at 1-cell stage), number and size of the blastomeres, an extent of fragmentation (at selected developmental time-points), and, at a blastocyst stage, presence of a blastocoel, a uniform, epithelial-like trophectoderm layer and size of an inner cell mass (Fig. 1B) (Ebner *et al.*, 2003; Ajduk and Zernicka-Goetz, 2013; Omidi *et al.*, 2017 and references therein).

Equipping a microscope with a time-lapse imaging system and then integrating it into a fully functional incubator has enabled embryo-safe recording of the cleavage divisions and provided access to information about developmental dynamics, so-called morphokinetics (Nakahara *et al.,* 2010; Pribenszky *et al.,* 2010; Meseguer *et al.,* 2011). Although time-lapse imaging involves periodic exposure to light, it is usually lower than that associated with a traditional morphology assessment, and most importantly enables embryo culture in stable, uninterrupted conditions. Morphokinetic parameters include absolute timings of the successive embryonic divisions, as well as relative timings, i.e. periods between the divisions, reflecting either duration of the cell cycle or synchronisation of the cleavage rounds. Time-lapse imaging also allows an assessment of morphological parameters, such as size of the blastomeres, number of nuclei in the blastomere, an extent of fragmentation, and occurrence of irregular cleavages. Although morphokinetics-based embryo assessment protocols have become increasingly popular in assisted reproduction over the last several years, it is still disputed whether they are indeed more reliable and effective than traditional scoring techniques (Kirkegaard *et al.,* 2015; Milewski and Ajduk, 2017 and references therein).

Time-lapse light microscopy can be also used to access information about dynamics of cellular processes, other than the cleavage divisions, that can be potentially useful as biomarkers of the embryonic quality. A good example here is movement of cytoplasm in fertilized oocytes: sperm-induced Ca^{2+} oscillations trigger rhythmic actomyosin-mediated spasms that translate to fast directional cytoplasmic movements, so called speed-peaks (Ajduk *et al.*, 2011; Swann *et al.*, 2012; Milewski *et al.*, 2018). Analysis of the cytoplasmic dynamics provides therefore information on functionality of the zygote cytoskeleton, especially its actomyosin component, and on the frequency of Ca^{2+} oscillations (Ajduk *et al.*, 2011). Both these properties are crucial for a proper embryonic development, with actomyosin cytoskeleton responsible for organelle trafficking and cellular divisions, and Ca^{2+} transients serving as a trigger for completion of meiosis, initiation of mitotic divisions, zona pellucida-mediated block to polyspermy and as a regulator of mitochondrial activity and gene expression in the embryos (Dumollard *et al.,* 2004; Ozil *et al.,* 2005, 2006; Campbell and Swann 2006; Ducibella *et al.,* 2006; Sun and Schatten 2006; D'Avino *et al.,* 2015).

Polarized light microscopy (PLM) is yet another way to enhance gamete assessment based on a morphological inspection. It allows visualisation of structures built of polymer-like units, such as metaphase spindle built of microtubules or zona pellucida built of chains of ZP proteins (Caamano *et al.*, 2010; Montag *et al.*, 2011; Omidi *et al.*, 2017). The partial alignment of molecular bonds or of submicroscopic particles leads to birefringence, which alters the state of passing polarized light (Box 2). When a polarized light beam enters a birefringent body, it is split into two beams with perpendicular vibration planes. PLM can be used to measure a relative change in phase between these two polarized beams, termed retardance, to quantify the birefringent property of the sample. The relative magnitude of light retardance is an indicator for density, high-order alignment or thickness of the birefringent object. Importantly, nowadays, due to advancements in polarization optics and image-processing, such measurements do not depend on the sample orientation (Oldenbourg and Mei, 1995).

Since PLM visualizes structure and localization of metaphase spindle in oocytes, it has been applied to assess meiotic maturity of oocytes. It has been also suggested to improve an outcome of nuclear transfer and intracytoplasmic sperm injection procedures. Moreover, PLM quantitatively distinguishes intrinsic structure of zona pellucida that has been implicated as yet another marker of oocyte developmental potential, as it reflects most likely quality of the follicular environment and course of the oocyte growth (Caamano *et al.*, 2010; Montag *et al.*, 2011; Omidi *et al.*, 2017 and references therein). Birefringence characterizes also sperm heads. In spermatozoa that underwent the acrosome reaction it is present only in the postacrosomal compartment, whereas in non-reacted spermatozoa - over the entire sperm head (Inoue, 1981; Baccetti, 2003). It has been proposed that birefringence

of sperm heads can be applied in assisted reproduction to select competent male gametes (Montag *et al.*, 2011; Omidi *et al.*, 2017 and references therein).

Neither standard light microscopy, nor PLM, is able to visualize detailed inner architecture of examined oocytes/embryos, nor has a high depth resolution. Harmonic generation microscopy (HGM), distinguishes, on the other hand, not only spindles and zona pellucida (via second harmonic generation), but also lipid droplets, nucleoli and membranous organelles such as Golgi apparatus, endoplasmic reticulum and mitochondria (via third harmonic generation) (Box 2; Hsieh *et al.*, 2008; Watanabe *et al.*, 2010; Thayil *et al.*, 2011; Kyvelidou *et al.*, 2011). HGM utilizes a nonlinear optical phenomenon, where a single photon with shorter wavelength (and doubled or tripled energy) is created from two or three low energy photons. In contrast to laser-induced fluorescence, HGM leaves no energy deposition in the sample: the emitted HGM photon energy is the same as the annihilated excitation photon energy (Sun *et al.*, 2004). Due to this energy-conservation characteristic HGM is considered non-invasive and therefore can be applied not only in research, but potentially also in a clinical setting. Moreover, it is compatible with a time-lapse imaging. Although it has been used to image *Drosophila*, zebrafish and mouse embryos (Sun *et al.*, 2004; Debarre *et al.*, 2006; Hsieh *et al.*, 2008; Watanabe *et al.*, 2010; Thayil *et al.*, 2011; Kyvelidou *et al.*, 2011), its usefulness in assisted reproduction has yet to be proven. Due to the abovementioned advantages and high imaging penetration depth (HGM utilizes near-infrared wavelengths), this microscopy method has become increasingly popular in other biomedical applications, including oncology and cardiology (Keikhosravi *et al.*, 2014; Weigelin *et al.*, 2016 and references therein).

Another fluorophore-free approach to provide 3D image of intracellular architecture is optical coherence microscopy (OCM), a recent incarnation of optical coherence tomography (OCT) with an enhanced resolution. OCT/OCM exploits the phenomenon that if polychromatic light is directed towards the sample and compared with the reference light, a useful signal appears only when the optical paths of the light scattered back from the sample and the reference light are almost equal. The first attempts of applying OCM (full field OCM that exploited so called time domain OCT with 2D CCD detector and mechanical scanning in z direction) to visualize mammalian gametes and early embryos revealed only very coarse intracellular structures, such as spindles and nuclei, or general morphology of embryos, such as shape and size of blastomeres at various cleavage stages or trophectoderm and inner cell mass in blastocysts (Xiao *et al.*, 2012; Zheng *et al.*, 2012, 2013a, 2013b; Zarnescu *et al.*, 2015). The main disadvantage of this approach was a relatively low imaging speed preventing a functional time-lapse imaging, as approximately 90 s were needed to acquire one 3D image. Another detection scheme, namely spectral OCT, where spectrometer is used to register spectral fringes carrying information about structure of the sample, has shortened this time to approximately 300 ms per one 3D volume. This increased imaging speed combined with a higher sensitivity of spectral OCT, as compared with a full field approach, have permitted significant improvement of the image quality. Additionally, combination of specifically designed trajectories of the scanning beam and signal processing protocols allowed to exploit the internal motion of cytoplasm in the imaged cells to effectively reduce the speckle noise, an obstacle typical for the OCT/OCM technique. Such optimized OCM system has provided 3D

high-resolution visualisations of the inner architecture of oocytes/embryos: nuclei with nucleoli, metaphase spindles, networks of ER and mitochondria. It is compatible with a time-lapse imaging, so it may be used to monitor and quantitatively analyse dynamic behaviour of these organelles over time (Karnowski *et al.*, 2017). This kind of structural and dynamic information is usually related to gamete/embryo quality and therefore may potentially serve as a quality predictor in IVF protocols. Its practical applicability requires however a further verification. Interestingly, OCM/OCT can be also used to image larger specimens, such as whole postimplantation embryos and foetuses (Larina *et al.*, 2011; Wu *et al.*, 2017), or cilia movement and sperm behaviour inside oviducts (Wang *et al.*, 2015, 2018; Wang and Larina, 2018).

Although, as described above, label-free methods provide a lot of valuable information regarding intracellular structure of gametes/embryos and, in combination with time-lapse imaging systems, dynamics of cellular processes, they cannot quantitatively identify chemical composition of the sample. One way to generate this kind of chemical specification without the need for external labelling is to exploit vibrational spectra of biomolecules. Vibrational resonances depend on the masses of the constituting atoms and their respective bond strengths. A typical vibrational spectrum therefore contains a large number of resonances related to the set of vibrational modes of the molecules reflecting the chemical composition of the sample (Carey, 1982). This principle has been applied in Raman spectro-microscopy (RSM). Light illuminating the sample interacts with its molecules, which leads to a shift in the photon energy. The shift reflects vibrational modes in the sample and in consequence its chemical composition. RSM utilizes light sources (usually lasers) in the visible wavelength range, and thus it delivers spatial resolutions comparable to those achievable in confocal fluorescence microscopy. However, Raman scattering (Box 2) is weak, and it can be disturbed by autofluorescence in the sample. This limitation has been overcome by anti-Stokes Raman scattering (CARS) microscopy, where signal intensity may be increased by orders of magnitude enabling label-free quantitative analysis of the chemical content (especially lipids) of living cells at high imaging speeds (Zumbusch *et al.*, 2013). RSM can be applied to examine chemical composition of oocytes and embryos (Bogliolo *et al.*, 2013; Davidson *et al.*, 2013; Bradley *et al.*, 2016; Jasensky *et al.*, 2016; Heraud *et al.*, 2017; Ishigaki *et al.*, 2017; Rusciano *et al.*, 2017), and therefore may provide insights into their metabolism and, in consequence, quality and developmental potential. However, similarly to HGM and OCM, RSM applicability in assisted reproduction needs confirmation, as it has not been yet fully tested in an IVF clinical setting.

In summary, a constant advancement in imaging techniques gradually extends our knowledge of cellular architecture and physiology. Many of those microscopic data have led to discoveries that have been already applied in medicine: imaging techniques utilized in basic research pointed out the most promising targets for novel diagnostic or treatment procedures. Reproductive biology and assisted reproduction are the perfect example here. Most of the parameters used in assessment of gamete/embryo quality in IVF clinics have strong biological merits and have been subjected to in-depth investigation with an aid of modern fluorescence microscopy. Only then, when those sensitive and effective but relatively invasive imaging methods reveal cellular features possessing a potential clinical significance, we can work on novel, non-invasive,

fluorophore-free imaging techniques capable of detecting those features and providing us with data both clinically useful and scientifically sound. It will be extremely interesting to see, how the gamete/embryo imaging toolkit will extend within the next decades.

References

AGOSTINHO A, KOUZNETSOVA A, HERNÁNDEZ-HERNÁNDEZ A, BERNHEM K, BLOM H, BRISMAR H and HÖÖG C (2018) Sexual dimorphism in the width of the mouse synaptonemal complex. *J Cell Sci* 131: jcs212548.

AJDUK A, ILOZUE T, WINDSOR S, YU Y, SERES KB, BOMPHREY RJ, TOM BD, SWANN K, THOMAS A, GRAHAM C and ZERNICKA –GOETZ M (2011) Rhythmic actomyosin driven contractions induced by sperm entry predict mammalian embryo viability. *Nat Comm* 2: 417.

AJDUK A and ZERNICKA-GOETZ M (2013) Quality control of embryo development. *Mol Aspects Med* 34: 903–918.

AJDUK A, BISWAS SHIVHARE S and ZERNICKA-GOETZ M (2014) The basal position of nuclei is one pre-requisite for asymmetric cell divisions in the early mouse embryo. *Dev Biol* 392: 133-140.

AJDUK A and ZERNICKA-GOETZ M (2016) Polarity and cell division orientation in the cleavage embryo: from worm to human. *Mol Hum Reprod* 22: 691-703.

AJDUK A, STRAUSS B, PINES J and ZERNICKA-GOETZ M (2017) Delayed APC/C activation extends the first mitosis of mouse embryos. *Sci Rep* 7: 9682.

AL-DOSSARY AA, BATHALA P, CAPLAN JL and MARTIN-DELEON PA (2015) Oviductosome-Sperm Membrane Interaction in Cargo Delivery. Detection of Fusion and Underlying Molecular Players Using Three-Dimensional Super-Resolution Structured Illumination Microscopy (SR-SIM). *J Biol Chem* 290: 17710–17723.

ALLEN JR, ROSS ST and DAVIDSON MW (2013). Single molecule localization microscopy for superresolution. *J Opt* 15: 094001.

ANANI S, BHAT S, HONMA-YAMANAKA N, KRAWCHUK D and YAMANAKA Y (2014) Initiation of Hippo signaling is linked to polarity rather than to cell position in the pre-implantation mouse embryo. *Development* 141: 2813-2824.

ANDREWS RE, GALILEO DS and MARTIN-DELEON PA (2015) Plasma membrane Ca2+-ATPase 4: interaction with constitutive nitric oxide synthases in human sperm and prostasomes which carry Ca2+/CaM dependent serine kinase. *Mol Hum Reprod* 21: 832-843.

AZOURY J, LEE KW, GEORGET V, RASSINIER P, LEADER B and VERLHAC MH (2008) Spindle positioning in mouse oocytes relies on a dynamic meshwork of actin filaments. *Curr Biol* 18: 1514-1519.

AZOURY J, LEE KW, GEORGET V, HIKAL P, VERLHAC MH (2011) Symmetry breaking in mouse oocytes requires transient F-actin meshwork destabilization. *Development* 138: 2903-2908.

BACCETTI B (2003) Microscopical advances in assisted reproduction. *J Submicrosc Cytol Pathol* 36: 333-339.

BALUCH DP and CAPCO DG (2008) GSK3β mediates acentromeric spindle stabilization by activated PKCζ. *Dev Biol* 317: 46-58.

BALUCH DP, KOENEMAN BA, HATCH KR, MCGAUGHEY RW and CAPCO DG (2004) PKC isotypes in post-activated and fertilized mouse eggs: association with the meiotic spindle. *Dev Biol* 274: 45-55

BARDELL D (2004) The Invention of the Microscope. *Bios* 75: 78-84.

BELLE M, GODEFROY D, COULY G, MALONE SA, COLLIER F, GIACOBINI P and CHEDOTAL A (2017) Tridimensional Visualization and Analysis of Early Human Development. *Cell* 169: 161–173.

BETZIG E, PATTERSON GH, SOUGRAT R, LINDWASSER OW, OLENYCH S, BONIFACINO JS, DAVIDSON MW, LIPPINCOTT-SCHWARTZ J and HESS HF (2006) Imaging intracellular fluorescent proteins at nanometer resolution. *Science* 313: 1642–1645.

BOGLIOLO L, MURRONE O, DI EMIDIO G, PICCININI M, ARIU F, LEDDA S and TATONE C (2013) Raman spectroscopy-based approach to detect aging-related oxidative damage in the mouse oocyte *J Assist Reprod Genet* 30: 877–882.

BOGOLYUBOVA I, STEIN G and BOGOLYUBOV D (2013) FRET analysis of interactions between actin and exon-exon-junction complex proteins in early mouse embryos. *Cell Tissue Res* 352: 277–285.

BOŠKOVIĆ A, EID A, PONTABRY J, ISHIUCHI T, SPIEGELHALTER C, RAGHU RAM EV, MESHORER E and TORRES-PADILLA ME (2014) Higher chromatin mobility supports totipotency and precedes pluripotency in vivo. *Genes Dev* 28: 1042-1047.

BRADLEY J, POPE I, MASIA F, SANUSI R, LANGBEIN W, SWANN K and BORRI P (2016) Quantitative imaging of lipids in live mouse oocytes and early embryos using CARS microscopy *Development* 143: 2238-2247.

CAAMANO JN, MUNOZ M, DIEZ C and GOMEZ E (2010) Polarized Light Microscopy in Mammalian Oocytes. *Reprod Dom Anim* 45: 49–56.

CAMPBELL K and SWANN K (2006) Ca2+ oscillations stimulate an ATP increase during fertilization of mouse eggs. *Dev Biol* 298: 225-233.

CANARIA CA AND LANSFORD R (2010) Advanced optical imaging in living embryos *Cell Mol Life Sci* 67: 3489–3497.

CAREY P (1982) Biochemical applications of Raman and resonance Raman spectroscopes. Academic Press, New York.

CENTONZE FROHLICH V (2008) Phase contrast and differential interference contrast (DIC) microscopy. *J Vis Exp* 17 doi: 10.3791/844.

CHUNG JJ, SHIM SH, EVERLEY RA, GYGI SP, ZHUANG X and CLAPHAM DE (2014) Structurally Distinct Ca2+ Signaling Domains of Sperm Flagella Orchestrate Tyrosine Phosphorylation and Motility. *Cell* 157: 808–822.

COX G (2011) Biological applications of second harmonic imaging. *Biophys Rev* 3: 131.

CRUZ M, GADEA B, GARRIDO N, PEDERSEN KS, MARTINEZ M, PEREZ-CANO I, MUNOZ M and MESEGUER M (2011) Embryo quality, blastocyst and ongoing pregnancy rates in oocyte donation patients whose embryos were monitored by time-lapse imaging. *J Assist Reprod Genet* 28: 569–573.

CUMMINS JM and WOODALL PF (1985) On mammalian sperm dimensions. *J Reprod Fert* 75: 153-175.

CUTHBERTSON KS and COBBOLD PH (1985) Phorbol ester and sperm activate mouse oocytes by inducing sustained oscillations in cell Ca2+. *Nature* 316: 541-542.

DAVIDSON B, MURRAY AA, ELFICK A and SPEARS N (2013) Raman Micro-Spectroscopy Can Be Used to Investigate the Developmental Stage of the Mouse Oocyte. *PLoS One* 8: e67972.

D'AVINO PP, GIANSANTI MG and PETRONCZKI M (2015) Cytokinesis in animal cells. *Cold Spring Harb Perspect Biol.* 7: a015834.

DEBARRE D, SUPATTO W, PENA AM, FABRE A, TORDJMANN T, COMBETTES L, SCHANNE-KLEIN MC and BEAUREPAIRE E (2006) Imaging lipid bodies in cells and tissues using third-harmonic generation microscopy. *Nat Methods* 3: 47-53.

DENK W, STRICKLER JH and WEBB WW (1990) Two-photon laser scanning fluorescence microscopy. *Science* 248: 73-76.

DUCIBELLA T, SCHULTZ RM and OZIL JP (2006) Role of calcium signals in early development. *Semin Cell Dev Biol* 17: 324-332.

DUMOLLARD R, MARANGOS P, FITZHARRIS G, SWANN K, DUCHEN M and CARROLL J (2004) Sperm-triggered [Ca2+] oscillations and Ca2+ homeostasis in the mouse egg have an absolute requirement for mitochondrial ATP production. *Development* 131: 3057-3067.

EBNER T, MOSER M, SOMMERGRUBER M and TEWS G (2003) Selection based on morphological assessment of oocytes and embryos at different stages of preimplantation development: a review. *Hum Reprod Update* 9: 251–262.

ETTINGER A and WITTMANN T (2014) Fluorescence live cell imaging. *Methods Cell Biol* 123: 77-94.

FIOLKA R (2014) Seeing more with structured illumination microscopy. *Methods Cell Biol* 123: 295-313.

GERVASI MG, XU X, CARBAJAL-GONZALEZ B, BUFFONE MG, VISCONTI PE and KRAPF D (2018) The actin cytoskeleton of the mouse sperm flagellum is organized in a helical structure. *J Cell Sci* 131: jcs215897.

GRÄF R, RIETDORF J and ZIMMERMANN T (2005) Live Cell Spinning Disk Microscopy. In: Rietdorf J. (eds) Microscopy Techniques. Springer, Berlin, Heidelberg.

Adv Biochem Engin/Biotechnol 95: 57– 75.

GRIFFIN J, EMERY BR, HUANG I, PETERSON CM and CARRELL DT (2006) Comparative analysis of follicle morphology and oocyte diameter in four mammalian species (mouse, hamster, pig, and human). *J Exp Clin Assist Reprod* 3: 2.

HEINTZMANN R and JOVIN TM (2002) Saturated patterned excitation microscopy— A concept for optical resolution improvement. *J Opt Soc Am A* 19: 1599–1609.

HEIN B, WILLIG KI and HELL SW (2008) Stimulated emission depletion (STED) nanoscopy of a fluorescent protein-labeled organelle inside a living cell. *Proc Natl Acad Sci USA* 105: 14271-14276.

HELL SW and WICHMANN J (1994). Breaking the diffraction resolution limit by stimulated emission- stimulated-emission-depletion fluorescence microscopy. *Opt Lett* 19: 780–782.

HELMCHEN F and DENK W (2005) Deep tissue two-photon microscopy. *Nat Methods* 2: 932–940.

HERAUD P, MARZEC KM, ZHANG QH, YUEN WS, CARROLL J and WOOD BR (2017) Label-free *in vivo* Raman microspectroscopic imaging of the macromolecular architecture of oocytes. *Sci Rep* 7: 8945.

HOELING BM, FERNANDEZ AD, HASKELL RC, HUANG E, MYERS WR, PETERSEN DC, UNGERSMA SE, WANG R, WILLIAMS ME, FRASER SE (2000) An optical coherence microscope for 3-dimensional imaging in developmental biology. *Opt Express* 6: 136-146.

HSIEH CS, CHEN SU, LEE YW, YANG YS and SUN CK (2008) Higher harmonic generation microscopy of *in vitro* cultured mammal oocytes and embryos. *Opt Express* 16: 11574-11588.

HUISKEN J, SWOGER J, DEL BENE F, WITTBRODT J and STELZER EHK (2004) Optical sectioning deep inside live embryos by selective plane illumination microscopy. *Science* 305: 1007–1009.

ICHIKAWA T, NAKAZATO K, KELLER PJ, KAJIURA-KOBAYASHI H, STELZER EH, MOCHIZUKI A and NONAKA S (2014) Live imaging and quantitative analysis of gastrulation in mouse embryos using light-sheet microscopy and 3D tracking tools. *Nat Protoc* 9: 575-585.

INOUE S (1981) Video image processing greatly enhances contrast, quality, and speed in polarization-based microscopy. *J Cell Biol* 89: 346–356.

INOUE S (2002) Polarization microscopy. *Curr Protoc Cell Biol* doi:10.1002/0471143030.cb0409s13.

ISHIGAKI M, HASHIMOTO K, SATO H and OZAKI Y (2017) Non-destructive monitoring of mouse embryo development and its qualitative evaluation at the molecular level using Raman spectroscopy. *Sci Rep* 7: 43942.

ITO C, YAMATOYA K and TOSHIMORI K (2015) Analysis of the complexity of the sperm acrosomal membrane by super-resolution stimulated emission depletion microscopy compared with transmission electron microscopy. *Microscopy (Oxf)* 64: 279-287.

JAMES PS, HENNESSY C, BERGE T and JONES R (2004) Compartmentalisation of the sperm plasma membrane: a FRAP, FLIP and SPFI analysis of putative diffusion barriers on the sperm head. *J Cell Sci* 117: 6485-6495.

JASENSKY J, BOUGHTON AP, KHMALADZE A, DING J, ZHANG C, SWAIN JE, SMITH GW, CHEN Z and SMITH GD (2016) Live-cell quantification and comparison of mammalian oocyte cytosolic lipid content between species, during development, and in relation to body composition using nonlinear vibrational microscopy *Analyst* 141: 4694–4706.

JONKMAN J, BROWN CM and COLE RW (2014) Quantitative confocal microscopy: Beyond a pretty picture. *Methods Cell Biol* 123: 113-134.

KARNOWSKI K, AJDUK A, WIELOCH B, TAMBORSKI S, KRAWIEC K, WOJTKOWSKI M and SZKULMOWSKI M (2017) Optical coherence microscopy as a novel, non-invasive method for the 4D live imaging of early mammalian embryos. *Sci Rep* 7: 4165.

KEIKHOSRAVI A, BREDFELDT JS, SAGAR AK and ELICEIRI KW (2014) Second-harmonic generation imaging of cancer. *Methods Cell Biol* 123: 531-546.

KELLER PJ and STELZER EH (2008) Quantitative *in vivo* imaging of entire embryos with Digital Scanned Laser Light Sheet Fluorescence Microscopy. *Curr Opin Neurobiol* 18: 624–632.

KIRKEGAARD K, AHLSTROM A, INGERSLEV HJ and HARDARSON T (2015) Choosing the best embryo by time lapse versus standard morphology. *Fertil Steril* 103: 323–332.

KREMERS GJ, GILBERT SG, CRANFILL PJ, DAVIDSON MW and PISTON DW.

(2011) Fluorescent proteins at a glance. *J Cell Sci* 124: 157-160.

KYVELIDOU C, TSEREVELAKIS GJ, FILIPPIDIS G, RANELLA A, KLEOVOULOU A, FOTAKIS C and ATHANASSAKIS I (2011) Following the course of pre-implantation embryo patterning by non-linear microscopy. *J Struct Biol* 176: 379-386.

LARINA IV, LARIN KV, JUSTICE MJ and DICKINSON ME (2011) Optical Coherence Tomography for live imaging of mammalian development. *Curr Opin Genet Dev* 21: 579–584.

LATRIVE A and BOCCARA AC (2011) *In vivo* and *in situ* cellular imaging full-field optical coherence tomography with a rigid endoscopic probe. *Biomed Opt Express* 2: 2897-2904.

LEUNG BO and CHOU KC (2011) Review of Super-Resolution Fluorescence Microscopy for Biology. *Appl Spectrosc* 65: 967-980.

LIU YZ, SHEMONSKI ND, ADIE SG, AHMAD A, BOWER AJ, CARNEY PS and BOPPART SA (2014) Computed optical interferometric tomography for high-speed volumetric cellular imaging. *Biomed Opt Express* 5: 2988-3000.

MADGWICK S, HANSEN DV, LEVASSEUR M, JACKSON PK and JONES KT (2006) Mouse Emi2 is required to enter meiosis II by reestablishing cyclin B1 during interkinesis. *J Cell Biol* 174: 791-801.

MANSER RC and HOUGHTON FD (2006) Ca2+-linked upregulation and mitochondrial production of nitric oxide in the mouse preimplantation embryo. *J Cell Sci* 119: 2048-2055.

DE MEDEIROS G, BALÁZS B and HUFNAGEL L (2016) Light-sheet imaging of mammalian development. *Semin Cell Dev Biol* 55: 148–155.

MESEGUER M, HERRERO J, TEJERA A, HILLIGSOE KM, RAMSING NB and REMOHI J (2011) The use of morphokinetics as a predictor of embryo implantation. *Hum Reprod* 26: 2658-2671.

MILEWSKI R and AJDUK A (2017) Time-lapse imaging of cleavage divisions in embryo quality assessment. *Reproduction* 154: R37–R53.

MILEWSKI R, SZPILA M and AJDUK A (2018) Dynamics of cytoplasm and cleavage divisions correlates with preimplantation embryo development. *Reproduction* 155: 1-14.

MONTAG M, KOSTER M, VAN DER VEN K and VAN DER VEN H (2011) Gamete competence assessment by polarizing optics in assisted reproduction. *Hum Reprod Update* 17: 654–666.

MORRIS SA, TEO RT, LI H, ROBSON P, GLOVER DM and ZERNICKA-GOETZ M (2010) Origin and formation of the first two distinct cell types of the inner cell mass in the mouse embryo. *Proc Natl Acad Sci USA* 107: 6364-6369.

MUKHERJEE S, JANSEN V, JIKELI JF, HAMZEH H, ALVAREZ L, DOMBROWSKI M, BALBACH M, STRUNKER T, SEIFERT R, KAUPP UB and WACHTEN D (2016) A novel biosensor to study cAMP dynamics in cilia and flagella. *eLife* 5: e14052.

NAKAHARA T, IWASE A, GOTO M, HARATA T, SUZUKI M, IENAGA M, KOBAYASHI H, TAKIKAWA S, MANABE S, KIKKAWA F and ANDO H (2010) Evaluation of the safety of time-lapse observations for human embryos. *J Assist Reprod Genet* 27: 93–96.

OLDENBOURG R (2013) Polarized light microscopy: principles and practice. *Cold Spring Harb Protoc* doi:10.1101/pdb.top078600

OLDENBOURG R and MEI G (1995) New polarized light microscope with precision universal compensator. *J Microsc* 180: 140-147.

OMIDI M, FARAMARZI A, AGHARAHIMI A and KHALILI MA (2017) Noninvasive imaging systems for gametes and embryo selection in IVF programs: a review. *J Microsc* 267: 253–264.

OOGA M, FULKA H, HASHIMOTO S, SUZUKI MG and AOKI F (2016) Analysis of chromatin structure in mouse preimplantation embryos by fluorescent recovery after photobleaching. *Epigenetics* 11: 85-94.

OOGA M and WAKAYAMA T (2017) FRAP analysis of chromatin looseness in mouse zygotes that allows full-term development. *PLoS One* 12: e0178255.

OREOPOULOS J, BERMAN R and BROWNE M (2014) Spinning-disk confocal microscopy: present technology and future trends. *Methods Cell Biol* 123: 153-175.

OZIL JP, BANREZES B, TOTH S, PAN H and SCHULTZ RM (2006) Ca2+ oscillatory pattern in fertilized mouse eggs affects gene expression and development to term. *Dev Biol* 300: 534-544.

OZIL JP, MARKOULAKI S, TOTH S, MATSON S, BANREZES B, KNOTT JG, SCHULTZ RM, HUNEAU D and DUCIBELLA T (2005) Egg activation events are regulated by the duration of a sustained [Ca2+]cyt signal in the mouse. *Dev Biol* 282: 39-54.

PARFITT DE and ZERNICKA-GOETZ M (2010) Epigenetic modification affecting expression of cell polarity and cell fate genes to regulate lineage specification in the early mouse embryo. *Mol Biol Cell* 21: 2649-2660.

PETRAN M, HADRAVSK M, EGGER MD and GALAMBOS R (1968) Tandem-scanning reflected light microscope. *J Opt Soc Am* 58: 661–664.

PLACHTA N, BOLLENBACH T, PEASE S, FRASER SE and PANTAZIS P (2011) Oct4 kinetics predict cell lineage patterning in the early mammalian embryo. *Nat Cell Biol* 13: 117-123.

PRAKASH K, FOURNIER D, REDL S, BEST G, BORSOS M, TIWARI VK, TACHIBANA-KONWALSKI K, KETTING RF, PAREKH SH, CREMER C and BIRK UJ (2015) Superresolution imaging reveals structurally distinct periodic patterns of chromatin along pachytene chromosomes. *Proc Natl Acad Sci USA* 112: 14635–14640.

PRIBENSZKY C, MATYAS S, KOVACS P, LOSONCZI E, ZADORI J and VAJTA G (2010) Pregnancy achieved by transfer of a single blastocyst selected by timelapse monitoring. *Reprod Biomed Online* 21: 533–536.

RUSCIANO G, DE CANDITIIS C, ZITO G, RUBESSA M, ROCA MS, CAROTENUTO R, SASSO A, GASPARRINI B (2017) Raman-microscopy investigation of vitrification-induced structural damages in mature bovine oocytes. *PLoS ONE* 12: e0177677.

RUST MJ, BATES M and ZHUANG XW (2006). Sub-diffraction-limit imaging by stochastic optical reconstruction microscopy (STORM). *Nat Methods* 3: 793–795.

SALMON ED and TRAN P (1998) High-resolution video-enhanced differential interference contrast (VE-DIC) light microscopy. *Methods Cell Biol* 56: 153-184

SAMARAGE CR, WHITE MD, ÁLVAREZ YD, FIERRO-GONZÁLEZ JC, HENON Y, JE-SUDASON EC, BISSIERE S, FOURAS A and PLACHTA N (2015) Cortical Tension Allocates the First Inner Cells of the Mammalian Embryo. *Dev Cell* 34: 435-447.

SANDERSON MJ, SMITH I, PARKER I and BOOTMAN MD (2014) Fluorescence Microscopy. *Cold Spring Harb Protoc* doi:10.1101/pdb.top071795

SANTI PA (2011). Light Sheet Fluorescence Microscopy: A Review. *J Histochem Cytochem* 59: 129-138.

SANTIQUET NW, DEVELLE Y, LAROCHE A, ROBERT C and RICHARD FJ (2012) Regulation of gap-junctional communication between cumulus cells during *in vitro* maturation in swine, a gap-FRAP study. *Biol Reprod* 87:46.

SAUNDERS CM, LARMAN MG, PARRINGTON J, COX LJ, ROYSE J, BLAYNEY LM, SWANN K and LAI FA (2002) PLC zeta: a sperm-specific trigger of Ca(2+) oscillations in eggs and embryo development. *Development* 129: 3533-3544.

SCHRÖTER F, JAKOP U, TEICHMANN A, HARALAMPIEV I, TANNERT A, WIESNER B, MÜLLER P and MÜLLER K (2016) Lipid dynamics in boar sperm studied by advanced fluorescence imaging techniques. *Eur Biophys J* 45: 149-163.

SCHUH M and ELLENBERG J (2008) A new model for asymmetric spindle positioning in mouse oocytes. *Curr Biol* 18: 1986-1992.

SHARIF M, SILVA E, SHAH STA and MILLER DJ (2017) Redistribution of soluble N-ethylmaleimide-sensitive-factor attachment protein receptors in mouse sperm membranes prior to the acrosome reaction. *Biol Reprod* 96: 352–365.

SHIRAKAWA H, ITO M, SATO M, UMEZAWA Y and MIYAZAKI S (2006) Measurement of intracellular IP3 during Ca2+ oscillations in mouse eggs with GFP-based FRET probe. *Biochem Biophys Res Commun* 345: 781–788.

SHTENGEL G, WANG Y, ZHANG Z, GOH WI, HESS HF and KANCHANAWONG P (2014) Imaging cellular ultrastructure by PALM, iPALM, and correlative iPALM-EM. *Methods Cell Biol* 123: 273-294.

SHUHAIBAR LC, EGBERT JR, NORRIS RB, LAMPE PD, NIKOLAEV VO, THUN-EMANN M, WEN L, FEIL R and JAFFE LA (2015) Intercellular signaling via cyclic GMP diffusion through gap junctions restarts meiosis in mouse ovarian follicles *Proc Natl Acad Sci USA* 112: 5527–5532.

STRAUSS B, HARRISON A, COELHO PA, YATA K, ZERNICKA-GOETZ M and PINES J (2018) Cyclin B1 is essential for mitosis in mouse embryos, and its nuclear export sets the time for mitosis. *J Cell Biol* 217: 179-193.

STRNAD P, GUNTHER S, REICHMANN J, KRZIC U, BALAZS B, DE MEDEIROS G, NORLIN N, HIIRAGI T, HUFNAGEL L and ELLENBERG J (2016) Inverted light-sheet microscope for imaging mouse pre-implantation development. *Nat Methods* 13: 139-142.

SUN CK, CHU SW, CHEN SY, TSAI TH, LIU TM, LIN CY and TSAI HJ (2004) Higher harmonic generation microscopy for developmental biology. *J Struct Biol* 147: 19–30.

SUN QY and SCHATTEN H (2006) Regulation of dynamic events by microfilaments during oocyte maturation and fertilization. *Reproduction* 131: 193–205.

THAYIL A, WATANABE T, JESACHER A, WILSON T, SRINIVAS S and BOOTH M (2011) Long-term imaging of mouse embryos using adaptive harmonic generation microscopy. *J Biomed Opt* 16: 046018.

UDAN RS, PIAZZA VG, HSU CW, HADJANTONAKIS AK and DICKINSON ME (2014) Quantitative imaging of cell dynamics in mouse embryos using light-sheet microscopy. *Development* (2014) 141: 4406-4414.

VERVEER PJ, SWOGER J, PAMPALONI F, GREGER K, MARCELLO M and STEL-ZER EH (2007) High-resolution three-dimensional imaging of large specimens with light sheet-based microscopy. *Nat Methods* 4: 311-313.

VOIE AH, BURNS DH and SPELMAN FA (1993) Orthogonal-plane fluorescence optical sectioning: three dimensional imaging of macroscopic biological specimens. *J Microsc* 170: 229-236.

WANG S, BURTON JC, BEHRINGER RR and LARINA IV (2015) *In vivo* micro-scale tomography of ciliary behavior in the mammalian oviduct. *Sci Rep* 5: 13216.

WANG S and LARINA IV (2018) *In vivo* three-dimensional tracking of sperm behaviors in the mouse oviduct. *Development* 145: dev157685.

WANG S, SYED R, GRISHINA OA and LARINA IV (2018) Prolonged *in vivo* functional assessment of the mouse oviduct using optical coherence tomography through a dorsal imaging window. *J Biophotonics* 11: e201700316.

WATANABE T, THAYIL A, JESACHER A, GRIEVE K, DEBARRE D, WILSON T, BOOTH M and SRINIVAS S (2010) Characterisation of the dynamic behaviour of lipid droplets in the early mouse embryo using adaptive harmonic generation microscopy. *BMC Cell Biology* 11: 38.

WEBER M, MICKOLEIT M and HUISKEN J (2014) Light sheet microscopy. *Methods Cell Biol* 123: 193-215.

WEIGELIN B, BAKKER GJ and FRIEDL P (2016) Third harmonic generation microscopy of cells and tissue organization. *J Cell Sci* 129: 245-255.

WHITE MD, ZENKER J, BISSIERE S and PLACHTA N (2018) Instructions for Assembling the Early Mammalian Embryo. *Dev Cell* 45: 667-679.

WU C, LE H, RAN S, SINGH M, LARINA IV, MAYERICH D, DICKINSON ME and LARIN KV (2017) Comparison and combination of rotational imaging optical coherence tomography and selective plane illumination microscopy for embryonic study. *Biomed Opt Express* 8: 4629-4639.

XIAO JY, WANG B, LU GY, ZHU ZQ and HUANG YJ (2012) Imaging of oocyte development using ultrahigh-resolution full-field optical coherence tomography. *Appl. Opt* 51: 3650–3654.

YAMANAKA M, KAWANO S, FUJITA K, SMITH NI and KAWATA S (2008) Beyond the diffraction-limit biological imaging by saturated excitation microscopy. *J Biomed Opt* 13: 050507.

ZARNESCU L, LEUNG MC, ABEYTA M, SUDKAMP H, BAER T, BEHR B and ELLER-BEE AK (2015) Label-free characterization of vitrification-induced morphology changes in single-cell embryos with full-field optical coherence tomography. *J Biomed Opt* 20: 096004.

ZERNIKE F (1935) Das Phasenkontrastverfahren bei der mikroskopischen Beobachtung. *Phys Zeitschr* 36: 848–851.

ZHENG JG, LU D, CHEN T, WANG C, TIAN N, ZHAO F, HUO T, ZHANG N, CHEN D, MA W, SUN JL and XUE P (2012) Label-free subcellular 3D live imaging of preimplantation mouse embryos with full-field optical coherence tomography. *J Biomed Opt* 17: 070503.

ZHENG JG, HUO T, CHEN T, WANG C, ZHANG N, TIAN N, ZHAO F, LU D, CHEN D, MA W, SUN JL and XUE P (2013) Understanding three-dimensional spatial relationship between the mouse second polar body and first cleavage plane with full-field optical coherence tomography. *J Biomed Opt* 18: 10503.

ZHENG JG, HUO T, TIAN N, CHEN T, WANG C, ZHANG N, ZHAO F, LU D, CHEN D, MA W, SUN JL and XUE P (2013) Noninvasive three-dimensional live imaging methodology for the spindles at meiosis and mitosis. *J Biomed Opt* 18: 50505.

ZUMBUSCH A, LANGBEIN W and BORRI P (2013) Nonlinear vibrational microscopy applied to lipid biology. *Prog Lipid Res* 52: 615–632.

Further Related Reading, published previously in the *Int. J. Dev. Biol.*

Single-molecule, antibody-free fluorescent visualisation of replication tracts along barcoded DNA molecules
Francesco De Carli, Vincent Gaggioli, Gaël A. Millot and Olivier Hyrien
Int. J. Dev. Biol. (2016) 60: 297-304

From jellyfish to biosensors: the use of fluorescent proteins in plants
Ute Voss, Antoine Larrieu and Darren M. Wells
Int. J. Dev. Biol. (2013) 57: 525-533

Over 40 years of mentoring, educating, and researching in the world of oocytes
Catherine M.H. Combelles and David Albertini
Int. J. Dev. Biol. (2012) 56: 765-770
https://doi.org/10.1387/ijdb.120176cc

Oocyte ageing and its cellular basis
Ursula Eichenlaub-Ritter
Int. J. Dev. Biol. (2012) 56: 841-852
https://doi.org/10.1387/ijdb.120141ue

OCT4 and the acquisition of oocyte developmental competence during folliculogenesis
Maurizio Zuccotti, Valeria Merico, Martina Belli, Francesca Mulas, Lucia Sacchi, Blaz Zupan,
Carlo Alberto Redi, Alessandro Prigione, James Adjaye, Riccardo Bellazzi and Silvia Garagna
Int. J. Dev. Biol. (2012) 56: 853-858

Knowledge-based bioinformatics for the study of mammalian oocytes
Francesca Mulas, Lucia Sacchi, Lan Zagar, Silvia Garagna, Maurizio Zuccotti, Blaz Zupan
and Riccardo Bellazzi
Int. J. Dev. Biol. (2012) 56: 859-866

Frontiers in fluorescence microscopy
José Rino, José Braga, Ricardo Henriques and Maria Carmo-Fonseca
Int. J. Dev. Biol. (2009) 53: 1569-1579